JLB

PIVOTAL ADVANCE

Pivotal Advance: Invariant NKT cells reduce accumulation of inflammatory monocytes in the lungs and decrease immune-pathology during severe influenza A virus infection

Wai Ling Kok, Laura Denney,* Kambez Benam,* Suzanne Cole,* Colin Clelland,† Andrew J. McMichael,* and Ling-Pei Ho*,‡,1*

*MRC Human Immunology Unit, Weatherall Institute of Molecular Medicine, University of Oxford, United Kingdom; †Pathology Department, The John Radcliffe Hospital, Oxford, United Kingdom; and ‡Oxford Centre for Respiratory Medicine, Churchill Hospital, Oxford, United Kingdom

RECEIVED APRIL 5, 2011; REVISED AUGUST 22, 2011; ACCEPTED AUGUST 23, 2011. DOI: 10.1189/jlb.0411184

ABSTRACT

Little is known of how a strong immune response in the lungs is regulated to minimize tissue injury during severe influenza A virus (IAV) infection. Here, using a model of lethal, high-pathogenicity IAV infection, we first show that Ly6C^{hi}Ly6G^{-} inflammatory monocytes, and not neutrophils, are the main infiltrate in lungs of WT mice. Mice devoid of iNKT cells (Jα18$^{-/-}$ mice) have increased levels of inflammatory monocytes, which correlated with increased lung injury and mortality (but not viral load). Activation of iNKT cells correlated with reduction of MCP-1 levels and improved outcome. iNKT cells were able to selectively lyse infected, MCP-1-producing monocytes in vitro, in a CD1d-dependent process. Our study provides a detailed profile and kinetics of innate immune cells in the lungs during severe IAV infection, highlighting inflammatory monocytes as the major infiltrate and identifying a role for iNKT cells in control of these cells and lung immune-pathology. *J. Leukoc. Biol.* 91: 357–368; 2012.

Introduction

The cause of mortality in high-pathogenicity IAV is unclear. It is likely to involve strain-specific viral factors, such as the propensity of the 1918 IAV to induce host immune response genes associated with inflammation and cell death pathways [1], increased ability of the virus to replicate at high efficiency [2], and host factors, such as a disproportionate (or deficient) immune response. With a high viral load, the immune response is highly activated but can be ineffective and is often accompanied by severe tissue injury. Most of the damage is thought to relate to the innate rather than adaptive immunity, but it is clear that innate immune cells are also required to clear viruses. Macrophages, DCs, and NK cells are particularly critical in the initial control of virus, and they also contribute to regulation of the adaptive-immune response during IAV infection [3]. Less is known of the contribution of monocytes and neutrophils to protection, although both subsets seem crucial for survival in high-pathogenicity IAV infection. Neutrophil-deficient mice infected with the H5N1 IAV strain [4] and mice lacking MCP-1 (also known as CCL-2), a chemoattractant for monocytes, have a worse outcome [5] than wild-type (WT) mice. However, removal of components of the innate system also resulted in improved survival, as mice deficient in NOS II and TNF-α (both produced mainly by myeloid-derived cells in the lungs) [6] and CCR2 (receptor for MCP-1)-deficient mice showed decreased mortality when infected with IAV [7]. Therefore, appropriate regulation of innate cells appears key to an optimal innate immune response—one that provides maximal protection and minimal bystander tissue damage. Relatively little is known about how the innate immune response is regulated.

One potential mechanism of regulation could involve a group of cells with immune-regulatory properties, called iNKT cells. These are unique subset of T cells with an invariant T cell receptor (TCR) that recognizes self and foreign glycolipid, presented by CD1d, a nonpolymorphic, MHC I-like protein [8]. Upon activation, iNKT cells release a cascade of cytokines; they mature DCs, activate NK cells, and help polyclonal antibody secretion [8, 9]. iNKT cells can also induce adaptive TH1-biased immune responses required for effective control of viral pathogens [10] and optimal host response [11–13]. Mice

Abbreviations: αGC=α-galactosylceramide, FSC=forward-scatter, H1N1=human influenza A virus (A/PR8/34), HAU=HA unit(s), IAV=influenza A virus, iNKT cell=invariant natural killer T cell, KC=keratinocyte-derived chemokine, qPCR=quantitative PCR, SSC=side-scatter, TCID50=tissue-culture infectivity dose 50, TipDC=TNF-α-producing, iNOS-expressing DCs

The online version of this paper, found at www.jleukbio.org, includes supplemental information.

1. Correspondence: MRC Human Immunology Unit, Weatherall Institute of Molecular Medicine, Oxford University, Oxford OX3 9DS, UK. E-mail: ling-pei.ho@imm.ox.ac.uk

lacking iNKT cells have worse outcome in models of *Streptococcus pneumoniae*, *Pseudomonas aeruginosa*, and *Chlamydia pneumonia* infections, Herpes simplex virus 1 and 2, murine CMV, lymphocytic choriomeningitis virus, and respiratory syncytial virus [14]. The specific importance of iNKT cells in antiviral immunity is supported by existence of viral mechanisms to down-regulate CD1d, allowing pathogens to evade recognition by these cells [15, 16]. We and others [17, 18] have shown recently that iNKT cells enhanced the immune response, reduced viral load, and improved outcome in mild (nonlethal), resolving IAV infection. In our present study, we are less interested in immune protection, rather, in whether iNKT cells can reduce immune-pathology in a situation where the host defense is maximally activated.

We show here that in a high immune-pathology, IAV infection model, iNKT cells did not affect viral load but rather, reduced lung injury. We also demonstrate that in severe IAV infection, inflammatory monocytes were the dominant immune cells in the lungs. Without iNKT cells, MCP-1 levels and inflammatory monocytes increased locally in the lungs, leading to higher numbers of mature macrophages. iNKT cells were capable of (preferentially) lysing IAV-infected monocytes in a CD1d-dependent process in vitro. We suggest that this may be a mechanism for control of this population of cells and reduction of immune-pathology during severe IAV infection.

MATERIALS AND METHODS

Virus infection and mice

C57BL/6 mice were obtained from breeding pairs originally purchased from The Jackson Laboratory (Bar Harbor, ME, USA). Mice lacking the Jα18 TCR gene segment [19] were kindly provided by Professor Masuru Taniguchi (RIKEN, Japan) and have been backcrossed at least 12 times with the C57BL/6 WT mice. All mice were maintained at the Biomedical Services Unit at the John Radcliffe Hospital (Oxford, UK) and were used according to established institutional guidelines. H1N1 was kindly provided by Professor John Skehel from the National Institute of Medical Research, Mill Hill (London, UK), and was administered intranasally to mice using methods described previously [17]. αGC (2 μg; Alexis Biochemicals, Axxora, Nottingham, UK) or control (vehicle media for αGC) [17] was administered by i.p. injection at the point of viral challenge. BAL fluid was obtained using methods described previously [17]. All animals were used according to established University of Oxford institutional guidelines (Oxford, UK) under the authority of a UK Home Office project license.

Viral titers were determined by serial dilution of mouse lung homogenates and tested for infectivity of Madin-Darby Canine Kidney cells. Infectious viral titer was determined according to the Reed and Muench method to obtain the TCID50/pair of lungs [20].

Histology assessment was made of H&E-stained sections obtained from the ventral and basal areas of the right lung. This was performed by a histopathologist (C. Clelland), who was blinded to the status of the treatment.

Cytokine and chemokine proteins were measured in serum and BAL using the Bio-Plex mouse cytokine array system (Bio-Rad, Hercules, CA, USA), according to the manufacturer's instructions.

Flow cytometry and reagents

Freshly isolated BAL cells or splenocytes were incubated with antimouse CD16/32 (FcγIII/IIR) and then multistained with different combinations of CD3, CD4, CD8, GR1 (RB6-8C5 clone), CD11b, F4/80, Ly6G (1A8 clone), Ly6C (1G7.G10 clone), and αGC-CD1d dimer with appropriate isotype controls from the same companies. Some experiments were also stained concomitantly with αGC-CD1d tetramer (provided by Vincenzo Cerundolo, University of Oxford, UK) to ensure comparable staining between dimers and tetramers. All mAb were purchased from eBioscience (San Diego, CA, USA), apart from Ly6G and Ly6C (Miltenyi Biotec, UK). The dead cell population was determined initially in each organ population by Hoescht or 7-amino-actinomycin D staining. αGC-CD1d dimers were generated by loading of excess αGC (10 M) in solution with 8 μg soluble divalent human CD1d-IgG1 protein (BD PharMingen Biosciences, Oxford, UK), as described by the manufacturers and also, as described previously [17], followed by PE-coupled antimouse IgG1 (BD PharMingen Biosciences) at a 2:1 wt:wt ratio.

Intracelullar cytokine staining was performed as described previously [21].

Immunofluorescence and immunohistochemistry

Paraffin-embedded sections of whole lungs were stained with MCP-1 polyclonal antibody (ab7202) or rabbit polyclonal IgG (ab27478), both from Abcam (Cambridge, UK) using the Envision detection system (Dako, Cambridge, UK), according to the manufacturer's instruction. Antigen retrieval was performed using "target retrieval solution" (citrate buffer; Dako) for 20 min in the microwave.

BAL cells from FACS-sorted populations stained with CD11b, Ly6C, and Ly6G were cytospun onto glass slides and stained with hematoxylin solution (Sigma-Aldrich, UK) for 2 min.

Immunoflourescence of H1N1 IAV-infected Beas2B was performed using anti-HA mAb (a kind gift from Professor Alain Townsend, University of Oxford), with Alexa Fluor 488 goat antimouse IgG (Invitrogen, UK) as secondary mAb.

MCP-1 expression by qPCR

The iNKT clone was first cultured with αGC-loaded (or nonloaded) 721.221 (a human B cell line transfected with CD1d) in a 4-h coculture to provide activated or nonactivated iNKT cells. The iNK7 cells were then FACS-sorted from this coculture based on a FSC-SSC appearance so that they are untouched by antibody binding (for gating strategy and confirmation of purity of untouched iNKT cells, see Supplemental Fig. 4). Beas2B cells were infected with 400 HAU/mL of H1N1 and infections confirmed by positive expression of anti-HA mAb. Infected, adherent Beas2B cells were then cocultured with activated (vs. nonactivated) iNKT cells at a 1:1 Beas2B:iNKT cell number ratio.

RNA was extracted from Beas2B with the RNeasy mini kit (Qiagen, UK), according to the manufacturer's instruction, and reversed transcribed using the Superscript III RT enzyme (Invitrogen). The SYBR Green qPCR methods were used and described in Supplemental Methods online.

MCP-1 blocking experiments

$J\alpha18^{-/-}$ mice were infected with H1N1, as described above, and on Days 2, 3, and 4 after infection, 20 μg goat antimouse CCL2/MCP-1 (AF-479-NA) blocking antibody (R&D Systems, Minneapolis, MN, USA) was administered to these mice. On Days 2 and 4, blocking antibody was given i.v. and Day 3, i.p. Normal goat IgG (AB-108-C) (R&D Systems) was used as control.

Cell lines and clones

Beas2B and 721.221 cells were purchased from American Type Culture Collection (Manassas, VA, USA). CD1d-transfected 721.221 cells were a gift from Drs. Demin Li and Xiao Ning Xu (University of Oxford). iNKT clones were generated as described previously [21]. All cell lines and clones were tested for Mycoplasma infections.

Lysis and infection of human primary monocytes and neutrophils

Human monocytes were extracted from PBMCs isolated from normal individuals using CD14 MicroBeads (Miltenyi Biotec), according to conditions set out by the manufacturer. Infection of monocytes and neutrophils was performed by infecting 1×10^6 cells with 400 HAU/ml H1N1 in 200 μl

RPMI medium without serum but with 2 μg/ml trypsin (BD PharMingen Biosciences). After 1 h, cells were washed once and plated onto six-well plates with RPMI/10% (v/v) FCS or used immediately. Viral infectivity was confirmed with anti-HA mAb by flow cytometry.

Neutrophils were isolated from citrated blood by Dextran sedimentation of erythrocytes, followed by centrifugation over Percoll (Sigma-Aldrich) density gradient. Cell purities were determined by nuclear morphology of neutrophils on hematoxylin-stained cytospins.

^{51}Cr-release assay was performed as described previously [21], some with addition of 25 ug/ml final concentration CD1d blocking antibody (CD1d42; eBioscience) or a dose range of CD1d blocking antibody.

Statistical analysis

Differences in measured variables among groups of mice were determined using one-way ANOVA, where three groups of mice were compared at one time-point, and repeat measures ANOVA, where multiple time-points were used. Tukey test was used post-test to compare among groups. Survival curves were analyzed using a log-rank (Mantel-Cox) test. Student's *t* test was used when two groups were compared. Data are expressed as mean ± SEM. All statistical analyses were performed with the SPSS-Sigma Stat software. Significance was set at a *P* value of <0.05.

RESULTS

Lack of iNKT cells results in increased mortality in high-pathogenicity IAV infection

We first set up a murine model of a severe, lower respiratory tract infection using H1N1 IAV. Mice succumbed to severe lower respiratory tract pathology (Supplemental Fig. 1A). This model was distinct from the models used in our previous study [17] and that of De Santo and coworkers [18], which were models of mild and resolving IAV infection. In the murine model used in this paper, lung viral loads were three to four orders of magnitude higher than the mild model, mice lost more weight, and there was severe immune-pathology in the lungs, making this a model of highly active immune response with accompanying severe lung pathology (Supplemental Fig. 2A–C), rather than a model of immune protection (Supplemental Fig. 1B and ref. [17]).

In this IAV infection model, we found an accelerated rate of weight loss and fatality in iNKT-deficient (Jα18$^{-/-}$ mice) compared with WT mice (**Fig. 1A** and **B**). Conversely, mice that received αGC (which caused specific activation of iNKT cells) at the point of intranasal influenza virus inoculation demonstrated better disease course and survival rates (Fig. 1A and B).

To determine if these differences were a result of different viral loads, lungs were removed at defined time-points (Days 1, 3, and 5 after challenge), homogenized, and clarified for viral titer estimation. Lung viral loads were not significantly different among the three groups at any of these time-points (Fig. 1C). On Days 3 and 5, viral titers were also determined for the spleens and livers of mice to examine for potential viral dissemination. No virus was detected in these distant organs in any mice (data not shown).

Increased mortality in iNKT-deficient mice is caused by increased lung injury

As viral titers and dissemination were not different among the three groups of mice, we questioned whether increased lung immune-pathology could be the cause for the increased deaths in iNKT-deficient mice. On Day 5, freshly harvested lungs from these mice showed greater overt evidence of tissue injury, with widespread hemorrhagic and inflamed areas compared with WT-infected mice (Fig. 1D–G). Mice that received αGC had healthier, and better aerated and perfused areas in the lungs (Fig. 1F).

Signs of severe injury, characterized by completely denuded epithelium and squamous metaplasia of the bronchial epithelium, were also observed in iNKT-deficient mice but not in mice from any other groups (Fig. 1H and Supplemental Fig. 2D and E).

Ly6C^{hi}Ly6G^{-} inflammatory monocytes are the dominant cells in the lungs of WT mice during high-pathogenicity IAV infection

We first determined the subsets of innate immune cells involved in the immune response leading to lung pathology. Representative sections of formalin-preserved, nonlavaged lungs were prepared on Days 1, 3, and 5 from WT mice after IAV infection, stained with H&E, and analyzed blind by a histopathologist. We found complex and evolving changes in innate immune cell viability, size, and granularity in the lungs of WT mice during IAV infection (**Fig. 2A–C**). Cellular infiltrate to airway lumens of lungs on Day 1 was not significantly different from uninfected WT, and comprised mainly of resident alveolar macrophages (Fig. 2A), but by Day 3, large numbers of bronchi were filled with cells with a different morphology (Fig. 2B). Morphologically, these cells represented monocytes, macrophages, and neutrophils of different maturity (evident from size of cells, granules, vacuoles, and shape of nuclei). On Day 5, cells changed further in terms of size and vacuolation, and there were large numbers of cells with apoptotic bodies (Fig. 2C).

To delineate the identity of these cells, we used Ly6C and Ly6G staining. We found that staining of live cells revealed extra subsets in the lungs, not usually observed in the spleen (Fig. 2D). To analyze these changes further, we included further staining with CD3, CD11b, F4/80, FSC, and SSC and used a phenotyping strategy comprising six-color flow cytometry staining, gating on live/apoptosing cells only (Hoescht$^{neg/mid}$ cells), and use of multiple "all-but-one" mAb stainings in the six-color panel to discriminate between negative and positive staining populations on the FACS plot for live cells of different sizes and granularity. For example, to determine where to gate for positively staining F4/80 cells for Ly6C^{+}Ly6G^{+} cells, we stained the BAL cells with all but F4/80 (isotype control is used instead). With this method, we were able to accurately determine positive staining for cells with different sizes and granularity, which exhibited different degrees of autofluorescence.

Gating on CD11b^{+}CD3^{-} cells (Supplemental Fig. 3), Ly6G and Ly6C expression defined specific subsets of innate cells, CD11b^{hi}Ly6C^{hi}Ly6G^{-}, CD11b^{hi}Ly6C^{hi}Ly6G^{+}, CD11b^{hi}Ly6C^{hi}Ly6G^{+}F4/80^{+} (gates "ii", "iii", and "iv", respectively, in Fig. 2E and F), and CD11b^{hi}Ly6C^{mid}Ly6G^{+}F4/80^{-} (gate "v" in Fig. 2E and F). Gate "v" was found on FACS sorting to be the only subset with multilobulated-nucleated cells (100% of gate; Fig. 2G). We reasoned that on Day 3, gate "ii" contained inflammatory monocytes because of its FSC/SSC distribution, indicating

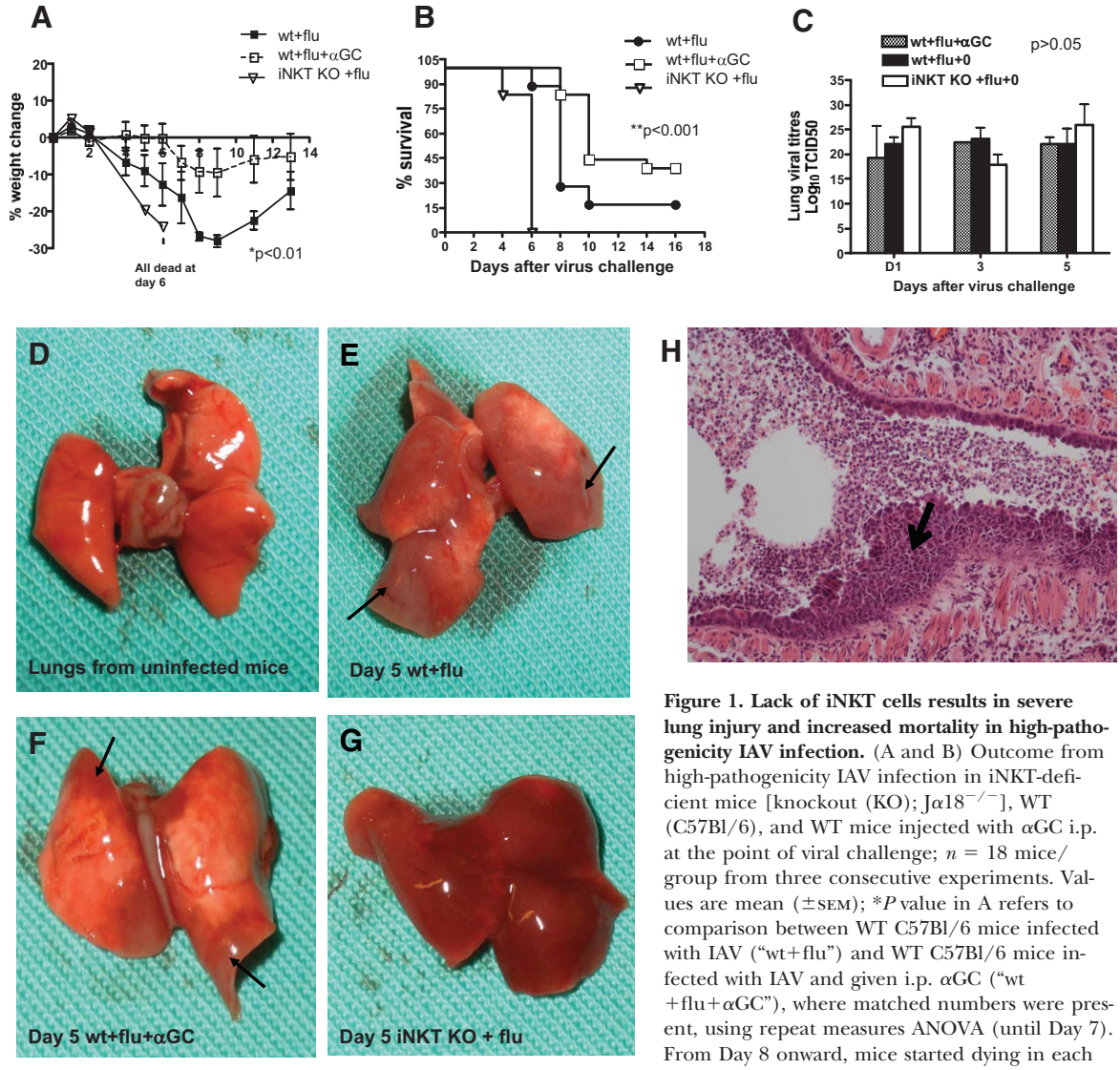

Figure 1. Lack of iNKT cells results in severe lung injury and increased mortality in high-pathogenicity IAV infection. (A and B) Outcome from high-pathogenicity IAV infection in iNKT-deficient mice [knockout (KO); J$\alpha 18^{-/-}$], WT (C57Bl/6), and WT mice injected with αGC i.p. at the point of viral challenge; $n = 18$ mice/group from three consecutive experiments. Values are mean (±SEM); *P value in A refers to comparison between WT C57Bl/6 mice infected with IAV ("wt+flu") and WT C57Bl/6 mice infected with IAV and given i.p. αGC ("wt+flu+αGC"), where matched numbers were present, using repeat measures ANOVA (until Day 7). From Day 8 onward, mice started dying in each group, and unbalanced numbers were present among the groups; in B, **$P < 0.001$ (log-rank Mantel-Cox test) for survival curve among the three groups. (C) Viral titers in homogenized lungs, measured as TCID50. (D–G) Freshly isolated lungs from mice killed on Day 5 after infection, showing areas of injury, worst in iNKT-deficient mice (G). The photographs are representative of 12 mice in each group. Arrows point to inflamed, poorly perfused, injured areas of lungs. iNKT-deficient mice showed widespread and frankly hemorrhagic areas (G). (H) H&E section from an iNKT-deficient mouse on Day 5 after infection, showing presence of respiratory tract infiltrate from iNKT-deficient mice, and areas of squamous metaplasia (arrow), the latter not observed in other groups of mice (see also Supplemental Fig. 2D and E).

that they were small but increasingly complex or granular cells. Gate "iii" had larger and more complex cells, which had the highest F4/80 expression, whereas gate "iv" was likely to be an extension of gate "ii", making gates "iii" and "iv" macrophages, and differentiating monocytes respectively. Gate "vi" comprised degranulating cells, which were also Hoescht^{mid} (Fig. 2G). By Day 5, there was a slight shift in the FSC/SSC of these Ly6G$^{+/-}$Ly6C$^{+/-}$ subsets, and gates "ii", "iii", and "iv" had greater proportions of more complex cells, likely signifying maturing of these cells with acquisition of larger vacuoles.

These staining panels demonstrate that the inflammatory monocyte-macrophage continuum was the dominant cell group in lungs of IAV-infected WT mice (**Figs.** 2E and F and **3C–E**). The neutrophils (gate "v") were the next-largest population, but in terms of absolute numbers, they were fourfold less than the inflammatory monocytes (Figs. 2E and F and 3C–E). None of the CD11b^{hi}Ly6C^{hi}Ly6G$^{+/-}$ cells were CD11c^{+} on Day 3, but up to 50% of the cells gained CD11c expression by Day 5 (Fig. 2H). We found no CD115 expression in any of the BAL cellular infiltrate, although CD115 was expressed in concomitant staining of spleen Ly6C^{+} cells (data not shown). We did not examine iNOS and TNF expression in these cells, but by the lack of CD11c expression in any of these cells on Day 3 (Fig. 2H), it was unlikely that the Ly6C^{hi} cells on Day 3 were TipDCs.

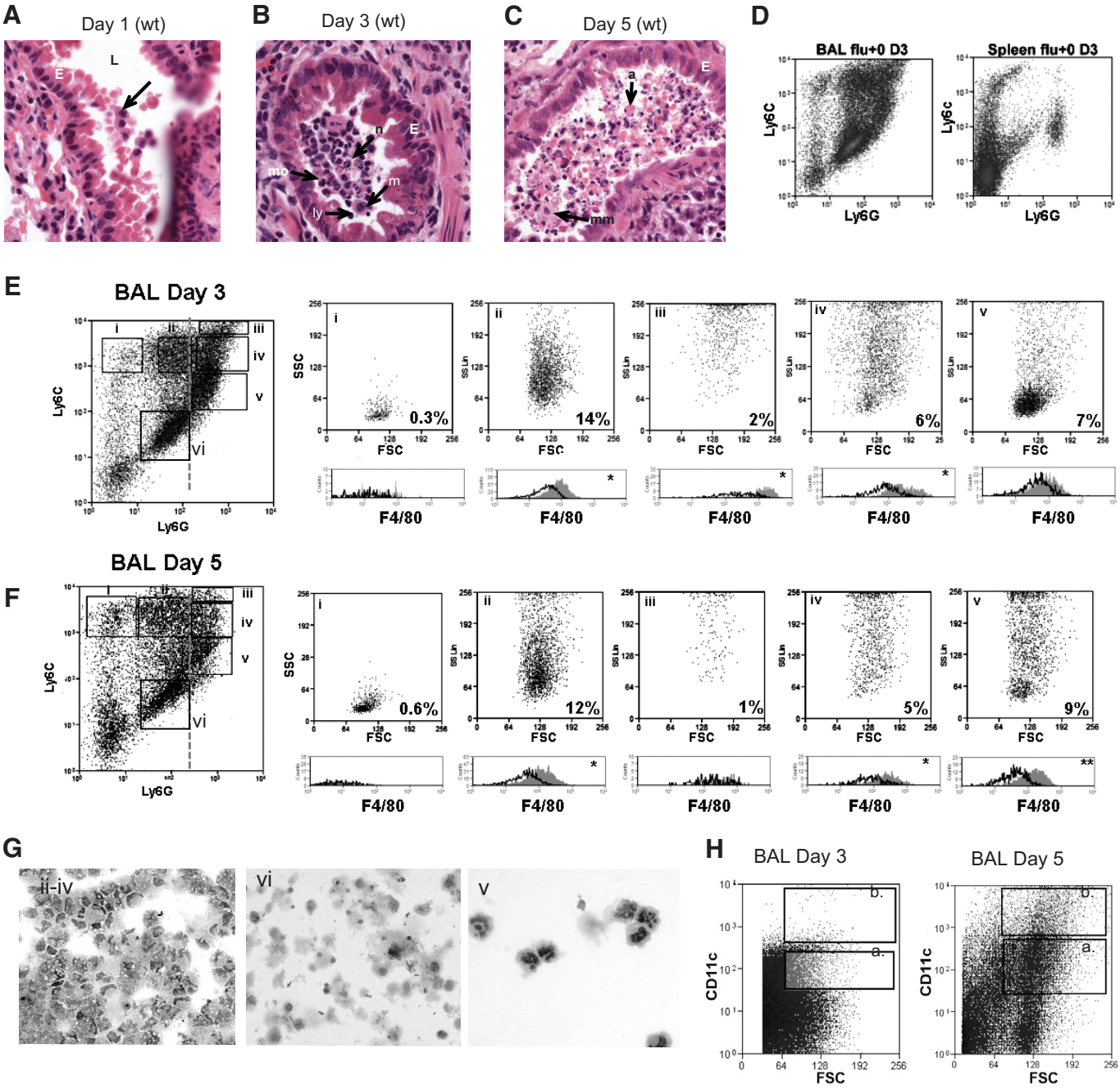

Figure 2. Innate immune cells in the lungs of WT mice during lethal IAV infection. (A–C) Representative H&E sections (×400) of paraffin-embedded lungs from WT mice on Days 1, 3, and 5 after IAV infection, demonstrating complex changes in morphology and types of cells within lumen of respiratory tracts during IAV infection. Arrow, resident alveolar macrophage; L, lumen of bronchus; E, bronchial epithelium; mo, monocytes; n, neutrophils; m, macrophage; ly, lymphocyte; a, cell with apoptotic bodies; mm, mature macrophage ready for degranulation. (D) Ly6C-Ly6G staining of $CD3^-$ cells in BAL and splenocytes on Day 3 after IAV challenge for WT mice. (E and F) FACS plots of BAL cells from IAV-infected WT mice, gated on $CD3^-$ cells, with Ly6C, Ly6G, and F4/80 staining of cells and their FSC/SSC profiles. Percent refers to proportion of $CD3^-CD11b^+$ cells. Broken line refers to division between positive and negative staining for Ly6G. Histograms are F4/80 staining for each individual gate ("i"–"v"; gray) against isotype control (unfilled histogram curves). Representative plot shown for $n = 6$ mice. (G) Hematoxylin staining of cells FACS-sorted from gates "ii" to "vi" show that "v" cells are multinucleated; "ii"–"iv" cells are a mixture of granular, vacuolated, with some multinucleated (representative figure shown); and "vi" cells are degranulated or dying cells and make up an average 55% of gated cells. (H) CD11c expression of all live ($Hoescht^{neg}$) cells in BAL on Days 3 and 5 after IAV infection, showing barely any CD11c staining on Day 3 but increase in $CD11c^{mid}$ (gate "a") and $CD11c^{hi}$ (gate "b") staining by Day 5.

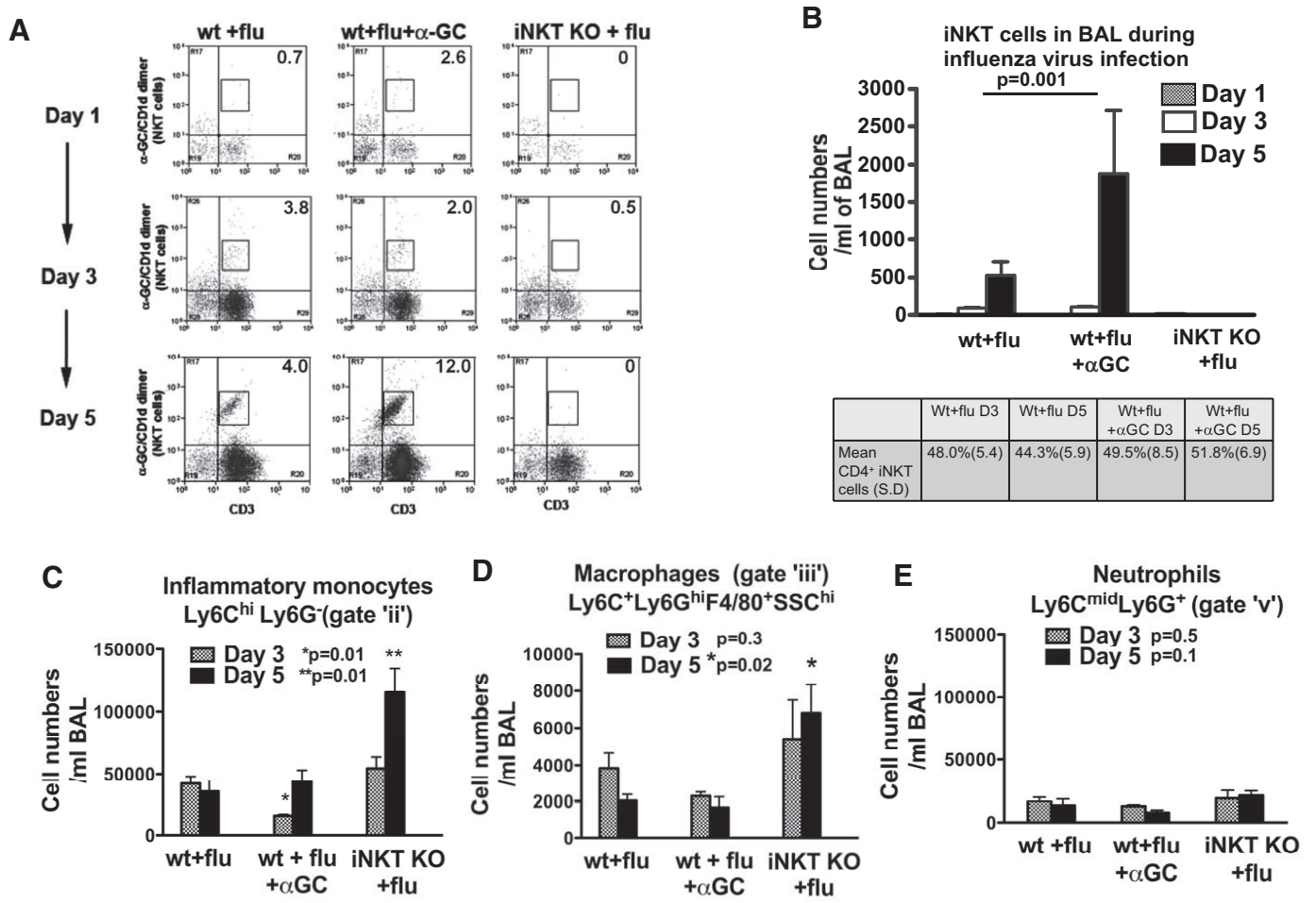

Figure 3. iNKT cells influence innate cellular infiltrate to lungs during lethal IAV infection. (A) Flow cytometry identification of iNKT cells in BAL-derived cells using an αGC-loaded CD1d dimer. FACS plots are gated on mononuclear cells. Percent is proportion of $CD3^+$ cells. Days 1, 3, and 5 refer to days after infection with IAV (basic controls for FACS staining shown in Supplemental Fig. 4C). (B) Absolute numbers of iNKT cells in BAL for the three groups of mice. *P* value refers to difference in mean between wt+flu and wt+flu+αGC on Day 5, derived using Student's *t* test. Lower panel shows the proportion of iNKT cells expressing CD4 as a percent of total lung iNKT cells. There was no difference among the four columns ($P>0.05$ one-way ANOVA with Tukey post test to compare among groups). (C–E) Absolute cell counts for different subsets of cells in BAL of IAV-infected mice. *P* values refer to differences among the three groups on Days 3 or 5 (one-way ANOVA). Total of $n = 18$ mice/group from three independent experiments. Note difference in *y*-axis scales for macrophages and inflammatory monocytes.

iNKT-deficient mice have higher numbers of inflammatory monocytes and macrophages in the lungs, and activation of iNKT cells reduced numbers of inflammatory monocytes and tissue injury

We next questioned whether iNKT cells were observed in lungs of mice with lethal IAV infection and whether iNKT activation and deletion affected the different populations of innate immune cells in the lungs. We found iNKT cells in the lungs within 3 days of infection in WT mice, amplified in mice administered αGC (2 μg i.p. at the point of IAV inoculation), and absent, as expected, in $J\alpha18^{-/-}$ mice (Fig. 3A and B). Approximately one-half of these infiltrating iNKT cells was $CD4^+$ and the other, $CD4^-$. There was no difference in CD4 expression on iNKT cells between infected mice given αGC and control and between Days 3 and 5 of infection (Fig. 3B, lower panel).

iNKT-deficient mice showed higher levels of inflammatory monocytes and macrophages than WT on Day 5 (Fig. 3C and D) in the BAL. In contrast, mice that received αGC had lower levels of inflammatory monocytes on Day 3 and no increase in macrophages on Day 5. Neutrophils were not affected by absence or activation of iNKT cells (Fig. 3E).

These findings show that iNKT cells were involved in the control of the size of inflammatory monocyte and macrophage (but not neutrophil) populations in the lungs and that in the absence of iNKT cells, mice died more rapidly from lung injury.

MCP-1 levels in the lungs are disproportionately increased in iNKT-deficient mice

To explore the mechanism by which iNKT cells influenced inflammatory monocytes, we first examined the sequential

changes in a range of cytokines and chemokines in the lungs (BAL) and blood (serum) using the Bio-Plex cytokine bead array system (Bio-Rad). We found MCP-1 to be markedly elevated from Day 3 onward in lungs (BAL) of iNKT-deficient mice (**Fig. 4A**). In contrast to other cytokines and chemokines, BAL MCP-1 levels continued to rise in iNKT-deficient mice throughout infection, peaked at Day 5, just before death (fourfold increase over WT mice), and were increased disproportionately compared with other cytokines and chemokines (Fig. 4B). Notably, mice treated with αGC and possessing the highest amount of iNKT cells in the lungs had significantly lower BAL MCP-1 levels compared with untreated mice ($P=0.03$, Student's t test). MIP-2 (also known as CXCL-2) and IL-6 levels in BAL of iNKT-deficient mice were also elevated significantly but returned to normal by Day 5.

Levels of cytokines and chemokines in the paired BAL serum samples showed that these increases were focused to the site of inflammation (lungs). However, IL-4 and IFN-γ levels in the serum were raised on Day 1 in contrast to BAL. This is similar to findings observed before [17] and likely to be a result of rapid release of these cytokines from iNKT cells in the liver. TNF-α, MCP-1, MIP-2, and KC were also raised significantly in serum of αGC-treated mice compared with WT and iNKT-deficient mice on Day 1.

Administration of MCP-1 blocking antibody to iNKT-deficient mice reduced lung monocyte and macrophage numbers and lung injury and improved survival

To assess the contribution of high MCP-1 levels to mortality in IAV-infected, iNKT-deficient mice, we administered MCP-1 blocking antibody i.v. to these mice on Days 2, 3, and 4 after viral challenge, compared with injections of IgG isotype control. In two consecutive experiments, we found a reduction in mortality and weight loss for mice treated with the MCP-1 blocking antibody (Fig. 4C). These did not reach statistical significance, but the trend of change in both experiments was the same. This correlated with a modest reduction in $Ly6C^{hi}$ cells in the lungs and reduction in overt lung injury in treated mice (Fig. 4D and E).

iNKT cells do not affect MCP-1 expression by infected respiratory epithelium or inflammatory monocytes

To determine the source of MCP-1 in lungs of infected mice and therefore, the potential point of influence by iNKT cells, lung sections from iNKT-deficient and WT mice, 1, 3, and 5 days after IAV infection (±αGC administration), were examined for expression of MCP-1 by immunohistochemistry. BAL cells were also FACS-sorted into $Ly6C^{hi}Ly6G^{-}$ (inflammatory monocytes) and $Ly6C^{mid}Ly6G^{+}$ (neutrophils) cells and cytospun onto slides for determination of MCP-1 expression. We found strong MCP-1 expression on the respiratory epithelium of all infected mice from Day 1 onward, compared with uninfected mice (**Fig. 5A**). In the cytospins, inflammatory monocytes, but not neutrophils, showed strong MCP-1 staining on Days 3 and 5 (Fig. 5B). Qualitatively, there was no difference in the intensity or distribution of MCP-1 expression in the respiratory epithelium or inflammatory monocytes among the three groups of mice on any of the three time-points.

To examine whether iNKT cells have the capacity to reduce MCP-1 expression in either of these cell groups quantitatively, we cocultured a human respiratory epithelial cell line (Beas2B) with a well-characterized human iNKT clone ($CD4^{+}$ NKT clone, LH22) [21] and examined MCP-1 mRNA expression in the adherent, respiratory epithelial cell line by qPCR. At the 24th h, iNKT cells were washed off, and the adherent Beas2B cells were replenished with fresh media and allowed to secrete MCP-1 for another 24 h (to remove the contribution of MCP-1 from iNKT cells). Neither MCP-1 mRNA expression nor protein levels in supernatant were reduced after incubation with activated iNKT cells compared with controls (Fig. 5C and D). In fact, activated iNKT cells increased MCP-1 expression and protein levels from infected Beas2B cells in vitro.

We next examined whether iNKT cells affected the other source of MCP-1 production, the inflammatory monocytes. Proportion and intensity of MCP-1 expression by intracellular cytokine staining of $Ly6C^{hi}Ly6G^{-}$ cells in BAL of iNKT-deficient mice were not different compared with WT on Days 1, 3, and 5 after influenza virus infection (data not shown). Although intensity differences in intracellular cytokine staining would not detect small changes in monocyte MCP-1 production, the overall results suggest that increased levels of MCP-1 in the BAL of iNKT-deficient mice were not a result of the increased ability of monocyte or respiratory epithelium to produce MCP-1.

Activated iNKT cells preferentially lyse infected monocytes in vitro in a CD1d-dependent process

As iNKT cells do not appear to affect the level of MCP-1 expression in monocytes or epithelial cells, we hypothesize that in WT mice, iNKT cells directly reduced the number of MCP-1-producing inflammatory monocytes by lysing these cells and that IAV infection of these CD1d-bearing subsets makes them a target for iNKT cells. To examine this, we first analyzed this in vitro. As we found that ^{51}Cr labeling was poor for isolated spleen and BAL monocytes from mice (data not shown), we used primary human cells. Autologous human monocytes were isolated using CD14 MACS beads and used as target cells, and two well-characterized human iNKT clones ($CD4^{-}$, LH18; $CD4^{+}$, LH22) [21] were used as effector cells at 20:1, 10:1, and 5:1 E:T ratios in a 5-h standard ^{51}Cr-release assay. We found that $CD4^{-}$ iNKT cells (but not the $CD4^{+}$ iNKT cell clone) killed monocytes in a dose-dependent manner (Fig. 5E). There was abundant CD1d expression on these monocytes (Fig. 5E, inset), and lysis with the $CD4^{-}$ iNKT cell clone was CD1d-dependent, as coculture with CD1d blocking antibody reduced specific lysis significantly (Fig. 5E).

Next, we questioned whether there was differential lysis of infected versus noninfected monocytes and neutrophils. For this, autologous, IAV-infected or noninfected $CD14^{+}$ monocytes or neutrophils were used as target cells in a 5-h standard ^{51}Cr-release assay with $CD4^{-}$ iNKT cell clone (LH18) as effectors. Infection was confirmed by HA staining (Fig. 5F). We found that iNKT cells lysed infected monocytes but not in-

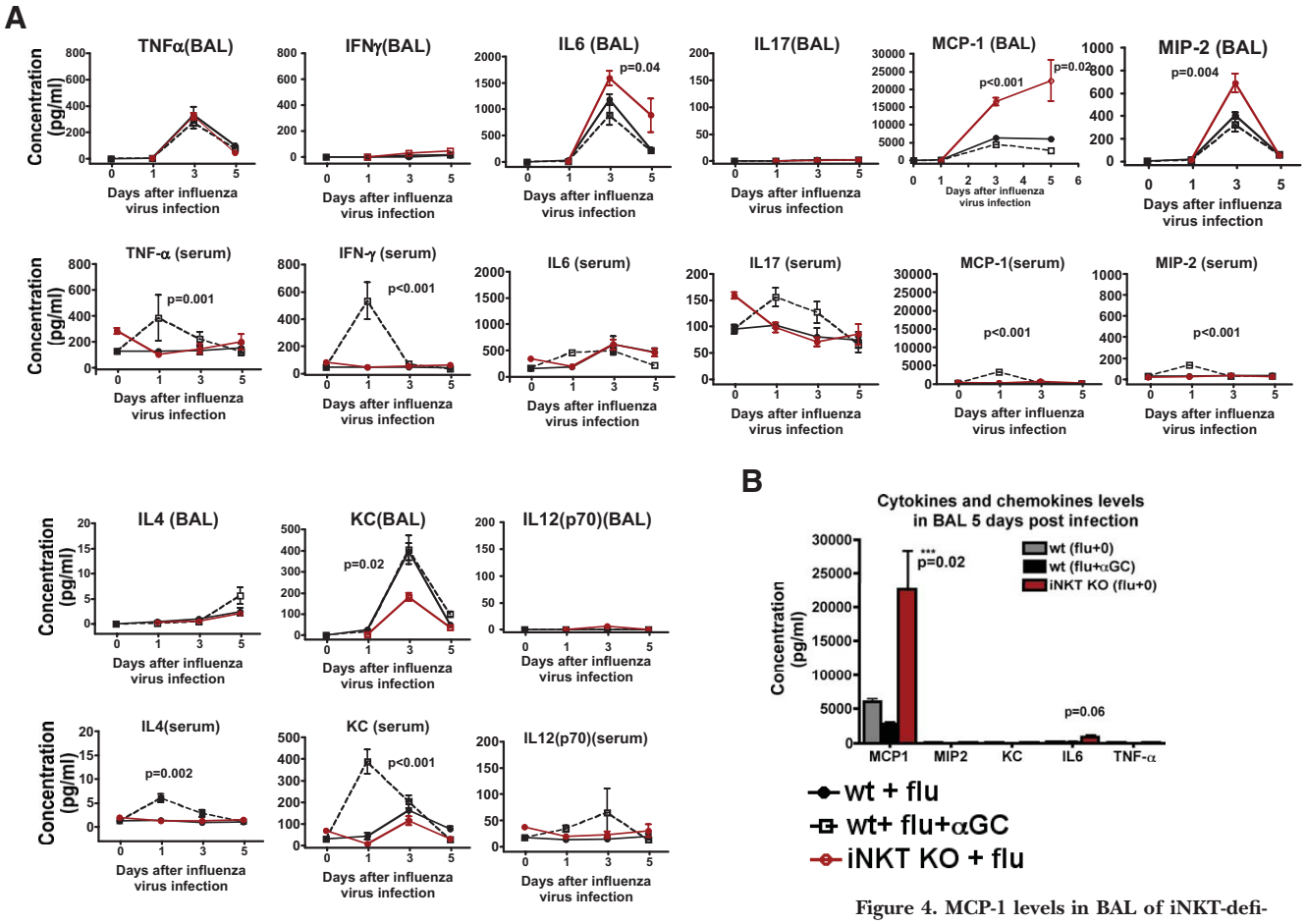

Figure 4. MCP-1 levels in BAL of iNKT-deficient mice are disproportionately increased and contribute to increased mortality. (A) BAL and serum levels for cytokines and chemokines, obtained on three time-points during IAV infection for the three groups of mice, $n = 6–9$ mice/group, from two consecutive experiments. Time-points with statistically significant different values were denoted by P values, which refer to comparison among the groups at the stated time-points, using one-way ANOVA. (B) Mean ($\pm$SEM) of five selected chemokine and cytokine levels in BAL, showing grossly elevated levels of MCP-1 in iNKT-deficient mice compared with the other two groups of mice and compared with other potentially immune-pathogenic chemokines and cytokines. P value refers to comparison among the three groups (one-way ANOVA). (C) Survival curves for iNKT-deficient mice infected with IAV and administered 20 μg anti-MCP-1 neutralizing antibodies (filled, red squares) on Days 2, 3, and 4 (arrows) or isotype control (□); $n = 10$/group in total. (D) Frequency of CD11b$^+$ Ly6C^{hi} cells in BAL of these mice on Day 5. (E) Gross appearance of lungs harvested from iNKT-deficient mice administered with 20 μg anti-MCP-1 neutralizing antibody versus control, showing greater areas of hemorrhagic damage (arrows). (F) Weight change in mice given anti-MCP-1 neutralizing antibody versus control. P value refers to comparison between the two groups.

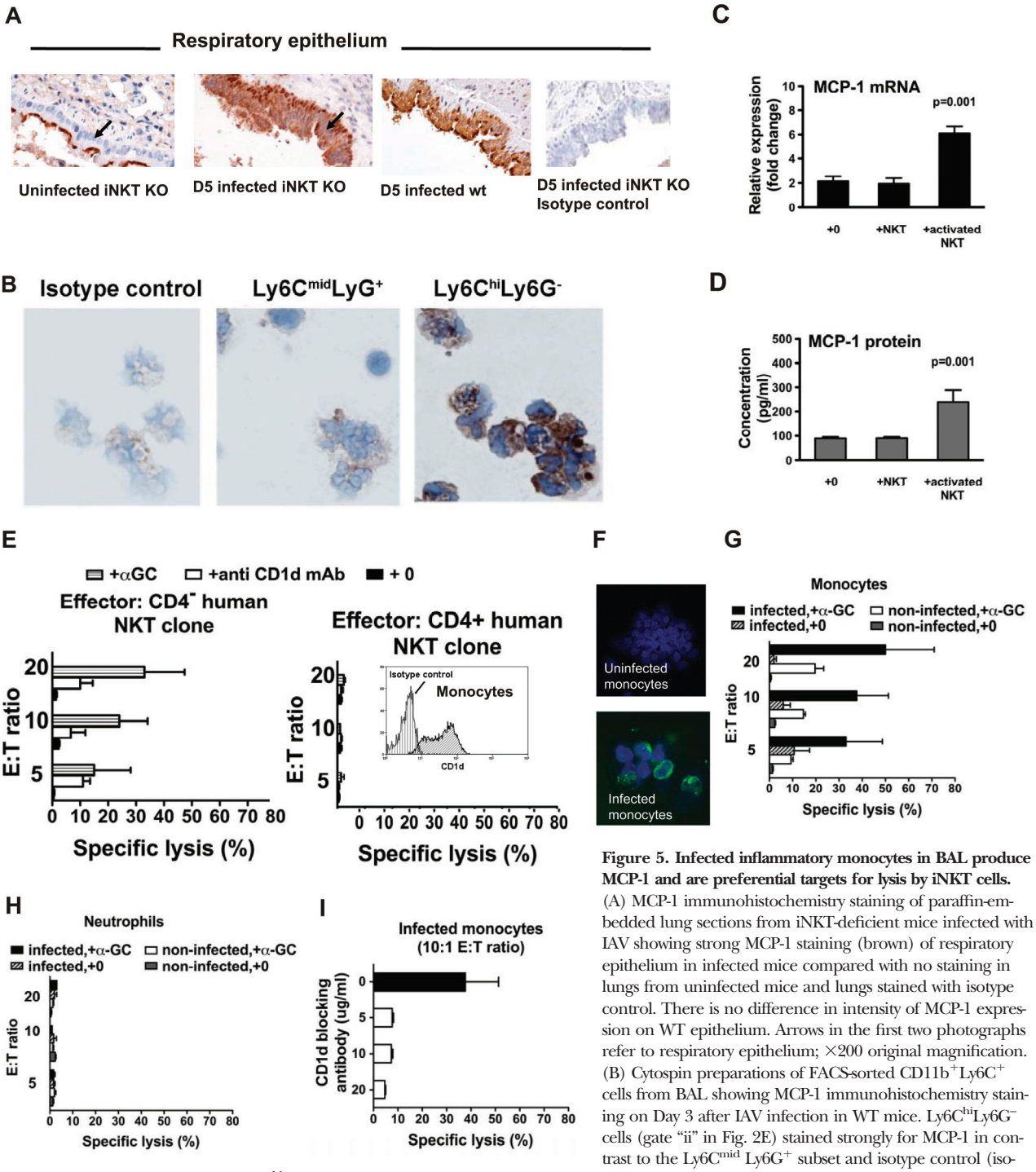

Figure 5. Infected inflammatory monocytes in BAL produce MCP-1 and are preferential targets for lysis by iNKT cells. (A) MCP-1 immunohistochemistry staining of paraffin-embedded lung sections from iNKT-deficient mice infected with IAV showing strong MCP-1 staining (brown) of respiratory epithelium in infected mice compared with no staining in lungs from uninfected mice and lungs stained with isotype control. There is no difference in intensity of MCP-1 expression on WT epithelium. Arrows in the first two photographs refer to respiratory epithelium; ×200 original magnification. (B) Cytospin preparations of FACS-sorted $CD11b^+Ly6C^+$ cells from BAL showing MCP-1 immunohistochemistry staining on Day 3 after IAV infection in WT mice. $Ly6C^{hi}Ly6G^-$ cells (gate "ii" in Fig. 2E) stained strongly for MCP-1 in contrast to the $Ly6C^{mid}$ $Ly6G^+$ subset and isotype control (isotype control staining shown is for $Ly6C^{hi}Ly6G^-$ cells; all ×400 original magnification). (C) Relative expression of MCP-1 mRNA by qPCR showing increased (rather than suppression of) MCP-1 expression by IAV-infected Beas2B cells with addition of αGC-activated iNKT clones ("+activated NKT") to the coculture, in contrast to when no iNKT clones ("+0") or when nonactivated iNKT ("+NKT") clones were added. Results for the 24th-h time-point are shown. (D) Similar results were observed with MCP-1 protein measured using the Bio-Plex mouse cytokine array system in the supernatant over a 24-h period after iNKT cells were removed at the 24th h. *P* value refers to comparison among the three conditions (one-way ANOVA). (E) Five-hour ^{51}Cr-release assays showing specific lysis of $CD14^+$ MACS bead-derived human monocytes by iNKT clones. Lysis required αGC ("+αGC" vs. +0) and was reduced with addition of 25 ug/ml of CD1d blocking antibody. (Inset) Histogram shows CD1d expression on monocytes used for the experiment. Error bars, SEM; mean of $n = 3$ experiments, each with duplicate wells. (F) Immunofluorescent HA staining (green) of $CD14^+$ monocytes after IAV infection (lower panel) compared with uninfected cells (upper panel). (G–I) αGC-activated $CD4^-$ iNKT clones lysed IAV-infected human monocytes more efficiently (solid bars) than noninfected monocytes (open bars) in a 5-h ^{51}Cr-release assay. iNKT clones were not able to lyse infected or noninfected neutrophils. At a 10:1 E:T ratio, a concomitant ^{51}Cr-release assay showed that addition of CD1d blocking antibody reduced the ability of $CD4^-$ iNKT clones to lyse infected monocytes in a dose-dependent manner.

fected neutrophils (Fig. 5G and H), and infected monocytes were lysed more efficiently than noninfected monocytes (Fig. 5G). Lysis of infected monocytes was enhanced with addition of αGC and was dependent on CD1d (Fig. 5I). However, without αGC, iNKT cells also appeared able to lyse infected target cells, albeit at a comparatively modest level (Fig. 5G).

DISCUSSION

In this study, we show by careful immunophenotyping that inflammatory monocytes are a major component of the innate immune response in the lungs during high-pathogenicity IAV infection and that iNKT cells can reduce lung pathology by modulating the accumulation of inflammatory monocytes in the lungs. This is distinct from iNKT cells' contribution to immune protection during IAV infection, which is thought to be provided by reduced recruitment of "myeloid-derived suppressor cells", allowing increased proliferation of influenza virus-specific CD8 T cell responses with resultant reduction in viral titers and improved survival [17, 18]. In this lethal IAV model, the worse outcome in iNKT-deficient mice was caused by increased lung injury rather than higher viral load, suggesting that iNKT cells not only have a role in immune protection but also in controlling inflammation. Without iNKT cells, inflammatory monocytes accumulate in the lungs, likely driven by high MCP-1 production by infected respiratory epithelium and inflammatory monocytes in an autocrine manner.

At least two distinct circulating and splenic monocyte subsets are known in mice: Ly6C$^+$ (CX_3CR1^+; inflammatory) and Ly6C$^-$ (patrolling) monocytes [22]. Ly6C$^+$ inflammatory monocytes (the monocytes implicated in this study) are thought to be the precursors of inflammatory TipDCs [23, 24] and macrophages and also replenish the resident DC population in tissue. They are important in microbial infection, as TipDCs are required for clearance of several pathogens [25], including high-pathogenicity IAV [26]. In some studies, subsets of monocytes have been discriminated by expression of CD115 (M-CSF), which is crucial for development of monocytes [27], and in the mature form, monocytes coexpress Ly6C and CD115.These are thought to be the monocytes that are recruited to inflamed tissue and lymph nodes, as they also bear CCR2. Interestingly, no expression of CD115 was found in any of the Ly6C$^+$ monocytes in our study suggesting that these cells may have down-regulated CD115 in the rich lung milieu of cytokines, as shown in other studies [28].

The kinetics and differentiation of mononuclear phagocyte cells in the lungs during severe infection have not been studied in detail. Their identity is complex, as CD11b, Ly6G, and F4/80 are expressed by inflammatory monocytes, maturing macrophages, and neutrophils [29, 30] and overlap in their expression during different points of viral infection. The subset of cells that was increased specifically in iNKT-deficient mice were the Ly6C$^+$CD11b^{hi}CD11c$^-$ cells on Day 5, which are destined to differentiate to TipDCs and macrophages. This increase matches the increase in BAL MCP-1 levels on Day 5 in iNKT-deficient mice compared with WT mice. This group of cells is likely to be similar to the one highlighted by Auffray et al. [28] which are precursor cells to the expanded injurious population observed by Aldridge et al. [26] in H5N1-infected mice. These findings underline the potential for interaction between innate cell and iNKT cells during IAV infection and are supported further by a recent publication (ref. [31]; published during review process of this paper), which showed that IAV-infected Jα18$^{-/-}$ mice had lower numbers of OVA-specific CD103$^+$ DCs in the draining lymph nodes of lungs and that iNKT cells can influence maturation of these cells.

MCP-1 production from epithelial cells and monocytes is known in the literature [32], but little is understood of how this is controlled during inflammation. Our findings suggest that in WT mice, a mechanism exists to control MCP-1 levels in the lung, which is absent in iNKT-deficient mice. In addition, administration of MCP-1 blocking antibodies to iNKT-deficient mice reduced immune-pathology in the lungs, albeit only modestly. Mice lacking MCP-1 do not survive IAV infection [5], so in our study, the intention was to moderate the rise in MCP-1 with blocking antibodies rather than to ameliorate this beyond a point where monocyte numbers fell to the extent of compromising host defense. As a result, we were not surprised to observe only moderate reduction in inflammatory monocytes in the lungs and consequently, a modest reduction in mortality and weight loss when blocking antibodies were administered. Although the changes did not reach statistical significance, all modalities (survival, weight, lung appearance, inflammatory monocytes) altered toward improvement for these IAV-infected, iNKT-deficient mice; supporting (although not proving) our hypothesis that injury associated with iNKT cell deficiency can be modulated by reducing MCP-1 and inflammatory monocyte levels.

Against our expectation, iNKT cells did not have a dampening effect on MCP-1 production from a respiratory epithelial cell line. In fact, the opposite was observed (Fig. 5C and D). We think this may be a result of the excess production of IFN-γ by a high ratio of iNKT:epithelial cells (1:1). MCP-1 gene expression can be induced rapidly by IFN-γ [33]. However, in the in vivo study, IFN-γ was not significantly elevated in the BAL of αGC-administered mice (Fig. 4A); therefore, contribution of iNKT-produced IFN-γ to stimulation of MCP-1 production by epithelial cells in vivo is less likely. These studies, however, were performed using cell lines and representative iNKT cell clones and therefore, support rather than prove that iNKT cells do not reduce MCP-1 production from infected respiratory epithelium in vivo.

Fig. 5 suggests that a potential mechanism, by which iNKT cells control numbers of Ly6C$^+$ inflammatory monocytes, is by direct lysis of these cells. We and others [21] have shown that iNKT cells can lyse CD1d-bearing target cells such as DCs. To our knowledge, there has been no report of lysis of inflammatory monocytes by iNKT cells, although a recent study by Song et al. [34] showed that iNKT cells can kill tumor-associated macrophages pulsed with tumor antigens, and Yang et al. [35] showed that DCs can be lysed by iNKT clones. Interestingly, only one of the two iNKT clones (CD4$^-$ iNKT clone) was able to lyse monocytes. It is possible that CD4$^-$ cytolytic iNKT subsets are selectively activated by soluble factors associated with infected monocytes. In the infected mice, iNKT cells infiltrating the lungs comprised CD4-positive and -negative iNKT cells

(Fig. 3B) in almost equal proportions; therefore, involvement of $CD4^-$ iNKT cells in killing monocytes at the site of inflammation is a possibility. The requirement for αGC reflects the need for activation of iNKT cells, but how this occurs during IAV infection is unclear. There is increasing evidence that a glycolipid antigen (i.e., direct activation) is not an absolute requirement [36]. IL-12 and IL-18 are known to activate iNKT cells by amplifying the baseline signal provided by a bound self-lipid [9, 37]. Indeed, Fig. 5G suggests that at a low iNKT: monocyte ratio, iNKT cells alone (without αGC) were able to kill infected monocytes compared with noninfected ones. This could be a result of IL-12 produced by iNKT cells or monocytes, as shown by Brigl et al. [9], or expression of a self-glycolipid on monocytes after infection, although there is little precedence for the latter. As the lysis experiments were performed in vitro and with human (rather than ex vivo mouse) monocytes and iNKT cells, the possibility of this being a mechanism in vivo is an extrapolation. Other potential mechanisms include the ability of iNKT cells to produce anti-inflammatory cytokines such as IL-10 [38] or to modulate IL-10-producing cells [39]. However, we did not find detectable IL-10 levels in the BAL on any of the days after infection in any of the groups (data not shown). In addition, although we showed that lysis of monocytes was reduced with CD1d blockade in vitro, the requirement for CD1d in vivo was not addressed in this study. The scenario in vivo is likely to be more complex, with likely contribution from CD1d-dependent (as shown by reduction of inflammatory monocytes in the lungs when αGC was administered) and -independent processes.

It is also unclear how iNKT cells begin to target monocytes for killing, but our in vitro studies showed that infected monocytes are lysed more efficiently, providing a method with which iNKT cells select less-useful but still injurious monocytes to be killed.

In summary, our study shows that iNKT cells have a role in controlling the intensity of the innate immune response. The combined results from the two IAV infection models demonstrate how both immune amplification and suppressive roles of iNKT cells can come to fore under different settings. Our study suggests that iNKT cells could mediate this reduction in inflammation by selectively targeting infected inflammatory monocytes for lysis. It also highlights the key contribution of inflammatory monocytes to lung injury in high-pathogenicity IAV infection. This has direct implication in high-pathogenicity influenza virus infection in humans, as it provides a specific target for further investigation and possibly therapeutic manipulation to improve survival in severe IAV infections.

AUTHORSHIP

L-P.H. wrote the paper, conceived of the ideas, designed the experiments, and analyzed the data. W.L.K. carried out all of the experiments and was involved in design and analysis of experiments. L.D., S.C., and K.B. performed some parts of the experiment. C.C. analyzed all of the histopathological data. A.J.M. reviewed some of the data.

ACKNOWLEDGMENTS

The studies were funded by the Medical Research Council UK and the Department of Health. We thank Craig Waugh and Kevin Clark for expert FACS sorting.

REFERENCES

1. De Jong, M.D., Simmons, C.P., Thanh, T.T., Hien, V.M., Smith, G.J., Chau, T.N., Hoang, D.M., Chau, N.V., Khanh, T.H., Dong, V.C., Qui, P.T., Cam, B.V., Ha do, Q., Guan, Y., Peiris, J. S., Chinh, N. T., Hien, T. T., Farrar, J. (2006) Fatal outcome of human influenza A (H5N1) is associated with high viral load and hypercytokinemia. *Nat. Med.* **12,** 1203–1207.
2. Kash, J. C., Tumpey, T. M., Proll, S. C., Carter, V., Perwitasari, O., Thomas, M. J., Basler, C. F., Palese, P., Taubenberger, J. K., García-Sastre, A., Swayne, D. E., Katze, M. G. (2006) Genomic analysis of increased host immune and cell death responses induced by 1918 influenza virus. *Nature* **443,** 578–581.
3. McGill, J., Heusel, J. W., Legge, K. L. (2009) Innate immune control and regulation of influenza virus infections. *J. Leukoc. Biol.* **86,** 803–812.
4. Tumpey, T. M., García-Sastre, A., Taubenberger, J. K., Palese, P., Swayne, D. E., Pantin-Jackwood, M. J., Schultz-Cherry, S., Solórzano, A., Van Rooijen, N., Katz, J. M., Basler, C. F. (2005) Pathogenicity of influenza viruses with genes from the 1918 pandemic virus: functional roles of alveolar macrophages and neutrophils in limiting virus replication and. mortality in mice. *J. Virol.* **79,** 14933–14944.
5. Dessing, M. C., van der Sluijs, K. F., Florquin, S., van der Poll, T. (2007) Monocyte chemoattractant protein 1 contributes to an adequate immune response in influenza pneumonia. *Clin. Immunol.* **125,** 328–336.
6. Jayasekera, J. P., Vinuesa, C. G., Karupiah, G., King, N. J. (2006) Enhanced antiviral antibody secretion and attenuated immunopathology during influenza virus infection in nitric oxide synthase-2-deficient mice. *J. Gen. Virol.* **87,** 3361–3371.
7. Dawson, T. C., Beck, M. A., Kuziel, W. A., Henderson, F., Maeda, N. (2000) Contrasting effects of CCR5 and CCR2 deficiency in the pulmonary inflammatory response to influenza A virus. *Am. J. Pathol.* **156,** 1951–1959.
8. Godfrey, D. I., Stankovic, S., Baxter, A. G. (2010) Raising the NKT cell family. *Nat. Immunol.* **11,** 197–206.
9. Brigl, M., Bry, L., Kent, S. C., Gumperz, J. E., Brenner, M. B. (2003) Mechanism of CD1d restricted natural killer T cell activation during microbial infection. *Nat. Immunol.* **4,** 1230–1237.
10. Van Dommelen, S. L., Degli-Esposti, M. A. (2004) NKT cells and viral immunity. *Immunol. Cell Biol.* **82,** 332–341.
11. Guillonneau, C., Mintern, J. D., Hubert, F. X., Hurt, A. C., Besra, G. S., Porcelli, S., Barr, I. G., Doherty, P. C., Godfrey, D. I., Turner, S. J. (2009) Combined NKT cell activation and influenza virus vaccination boosts memory CTL generation and protective immunity. *Proc. Natl. Acad. Sci. USA* **106,** 3330–3335.
12. Kamijuku, H., Nagata, Y., Jiang, X., Ichinohe, T., Tashiro, T., Mori, K., Taniguchi, M., Hase, K., Ohno, H., Shimaoka, T., Yonehara, S., Odagiri, T., Tashiro, M., Sata, T., Hasegawa, H., Seino, K. I. (2008) Mechanism of NKT cell activation by intranasal coadministration of α-galactosylceramide, which can induce cross-protection against influenza viruses. *Mucosal Immunol.* **1,** 208–218.
13. Diana, J., Lehuen, A. (2009) NKT cells: friend or foe during viral infections? *Eur. J. Immunol.* **39,** 3283–3291.
14. Cohen, N. R., Garg, S., Brenner, M. B. (2009) Antigen presentation by CD1 lipids, T cells, and NKT cells in microbial immunity. *Adv. Immunol.* **102,** 1–94.
15. Lin, Y., Roberts, T. J., Spence, P. M., Brutkiewicz, R. R. (2005) Reduction in CD1d expression on dendritic cells and macrophages by an acute virus infection. *J. Leukoc. Biol.* **77,** 151–158.
16. Yuan, W., Dasgupta, A., Cresswell, P. (2006) Herpes simplex virus evades natural killer T cell recognition by suppressing CD1d recycling. *Nat. Immunol.* **7,** 835–842.
17. Ho, L. P., Denney, L., Luhn, K., Teoh, D., Clelland, C., McMichael, A. J. (2008) Activation of invariant NKT cells enhances the innate immune response and improves the disease course in influenza A virus infection. *Eur. J. Immunol.* **38,** 1913–1922.
18. De Santo, C., Salio, M., Masri, S. H., Lee, L. Y., Dong, T., Speak, A. O., Porubsky, S., Booth, S., Veerapen, N., Besra, G. S., Gröne, H. J., Platt, F. M., Zambon, M., Cerundolo, V. (2008) Invariant NKT cells reduce the immunosuppressive activity of influenza A virus-induced myeloid-derived suppressor cells in mice and humans. *J. Clin. Invest.* **118,** 4036–4048.
19. Cui, J., Shin, T., Kawano, T., Sato, H., Kondo, E., Toura, I., Kaneko, Y., Koseki, H., Kanno, M., Taniguchi, M. (1997) Requirement for Vα14 NKT cells in IL-12-mediated rejection of tumors. *Science* **278,** 1623–1626.
20. Moskophidis, D., Kioussis, D. (1998) Contribution of virus-specific CD8+ cytotoxic T cells to virus clearance or pathologic manifestations of influ-

enza virus infection in a T cell receptor transgenic mouse model. *J. Exp. Med.* **188,** 223–232.
21. Ho, L. P., Urban, B. C., Jones, L., Ogg, G. S., McMichael, A. J. (2004) CD4(–) CD8aa subset of CD1d-restricted NKT cells controls T cell expansion. *J. Immunol.* **172,** 7350–7358.
22. Geissmann, F., Jung, S., Littman, D. R. (2003) Blood monocytes consist of two principal subsets with distinct migratory properties. *Immunity* **19,** 71–82.
23. Serbina, N. V., Salazar-Mather, T. P., Biron, C. A., Kuziel, W. A., Pamer, E. G. (2003) TNF/iNOS-producing dendritic cells mediate innate immune defense against bacterial infection. *Immunity* **19,** 59–70.
24. Dai, X. M., Ryan, G. R., Hapel, A. J., Dominguez, M. G., Russell, R. G., Kapp, S., Sylvestre, V., Stanley, E. R. (2002) Targeted disruption of the mouse colony-stimulating factor 1 receptor gene results in osteopetrosis, mononuclear phagocyte deficiency, increased primitive progenitor cell frequencies, and reproductive defects. *Blood* **99,** 111–120.
25. Serbina, N. V., Jia, T., Hohl, T. M., Pamer, E. G. (2008) Monocyte-mediated defense against microbial pathogens. *Annu. Rev. Immunol.* **26,** 421–452.
26. Aldridge, J. R., Moseley, C. E., Boltz, D. A., Negovetich, N. J., Reynolds, C., Franks, J., Brown, S. A., Doherty, P. C., Webster, R. G., Thomas, P. G. (2009) TNF/iNOS-producing dendritic cells are the necessary evil of lethal influenza virus infection. *Proc. Natl. Acad. Sci. USA* **106,** 5306–5311.
27. Auffray, C., Sieweke, M. H., Geissmann, F. (2009) Blood monocytes: development, heterogeneity and relationship with dendritic cells. *Annu. Rev. Immunol.* **27,** 669–692.
28. Auffray, C., Fogg, D. K., Narni-Mancinelli, E., Senechal, B., Trouillet, C., Saederup, N., Leemput, J., Bigot, K., Campisi, L., Abitbol, M., Molina, T., Charo, I., Hume, D. A., Cumano, A., Lauvau, G., Geissmann, F. (2009) CX3CR1+CD115+CD135+ common macrophage/DC precursors and the role of CX3CR1 in their response to inflammation. *J. Exp. Med.* **206,** 595–606.
29. Egan, C. E., Sukhumavasi, W., Bierly, A. L., Denkers, E. Y. (2008) Understanding the multiple functions of Gr-1(+) cell subpopulations during microbial infection. *Immunol. Res.* **40,** 35–48.
30. Gordon, S., Taylor, P. R. (2005) Monocyte and macrophage heterogeneity. *Nat. Rev. Immunol.* **5,** 953–964.
31. Paget, C., Ivanov, S., Fontaine, J., Blanc, F., Pichavant, M., Renneson, J., Bialecki, E., Pothlichet, J., Vendeville, C., Barba-Speath, G., Huerre, M. R., Faveeuw, C., Si-Tahar, M., Trottein, F. (2011) Potential role of invariant NKT cells in the control of pulmonary inflammation and CD8+ T cell response during acute influenza A virus H3N2 pneumonia. *J. Immunol.* **186,** 5590–5602.
32. Yadav, A., Saini, V., Arora, S. (2010) MCP-1: chemoattractant with a role beyond immunity: a review. *Clin. Chim. Acta* **411,** 1570–1579.
33. Valente, A. J., Xie, J. F., Abramova, M. A., Wenzel, U. O., Abboud, H. E., Graves, D. T. (1998) A complex element regulates IFN-stimulated monocyte chemoattractant protein-1 gene transcription. *J. Immunol.* **161,** 3719–3728.
34. Song, L., Asgharzadeh, S., Salo, J., Engell, K., Wu, H. W., Sposto, R., Ara, T., Silverman, A. M., DeClerck, Y. A., Seeger, R. C., Metelitsa, L. S. (2009) Vα24-invariant NKT cells mediate antitumor activity via killing of tumor-associated macrophages. *J. Clin. Invest.* **119,** 1524–1536.
35. Yang, O. O., Racke, F. K., Nguyen, P. T., Gausling, R., Severino, M. E., Horton, H. F., Byrne, M. C., Strominger, J. L., Wilson, S. B. (2000) CD1d on myeloid dendritic cells stimulates cytokine secretion from and cytolytic activity of V α 24J α Q T cells: a feedback mechanism for immune regulation. *J. Immunol.* **165,** 3756–3762.
36. Brigl, M., Brenner, M. B. (2010) How invariant natural killer T cells respond to infection by recognizing microbial or endogenous lipid antigens. *Semin. Immunol.* **22,** 79–86.
37. Leite-De-Moraes, M. C., Hameg, A., Arnould, A., Machavoine, F., Koezuka, Y., Schneider, E., Herbelin, A., Dy, M. (1999) A distinct IL-18-induced pathway to fully activate NK T lymphocytes independently from TCR engagement. *J. Immunol.* **163,** 5871–5876.
38. Gumperz, J. E., Miyake, S., Yamamura, T., Brenner, M. B. (2002) Functionally distinct subsets of CD1d-restricted natural killer T cells revealed by CD1d tetramer staining. *J. Exp. Med.* **195,** 625–636.
39. De Santo, C., Arscott, R., Booth, S., Karydis, I., Jones, M., Asher, R., Salio, M., Middleton, M., Cerundolo, V. (2010) Invariant NKT cells modulate the suppressive activity of IL-10-secreting neutrophils differentiated with serum amyloid A. *Nat. Immunol.* **11,** 1039–1046.

KEY WORDS:
iNKT · chemokines · respiratory viruses · innate immune response · lung injury